Cent. Eur. J. Geosci. • 1(2) • 2009 • 219-226
DOI: 10.2478/v10085-009-0011-x

VERSITA

Central European Journal of **Geosciences**

Groundwater and soil geochemistry of the Eastern Kopaida region (Beotia, central Greece)

Research Article

Evangelos P. Tziritis*

National and Kapodistrian University of Athens, Faculty of Geology and Geoenvironment, University Campus, z.c. 15784, Zografou, Athens Greece

Received 5 March 2009; accepted 16 April 2009

Abstract: The Kopaida plain is a cultivated region of Eastern Greece, with specific characteristics related to the paleogeographic evolution and the changes in land use of the area. This study examines the geochemical conditions of the groundwater and soil, and the correlations between them. 70 samples (50 samples of groundwater and 20 samples of soil) were collected in order to asses the geochemical status and the major natural and manmade affecting processes in the region. Extended chemical analyses were carried out including the assessment of 28 parameters for groundwater and 13 for soil samples. The results revealed that groundwater geochemistry is influenced primary by natural processes such as the geological background, and secondary by manmade impact mainly deriving from the extended use of Nitrogen-fertilizers and the over-exploitation of boreholes. Soil geochemistry is influenced exclusively by natural processes, such as weathering of the prevailing geological formations. Chemical analyses and the statistical processing of data revealed that the major factor for the geochemical status of soils is the weathering of the karstic substrate, as well as the existing lateritic horizons and a weak sulfide mineralization.

Keywords: Kopaida • geochemistry • groundwater • soil • environment

1. Introduction

The Kopaida plain is a great polje (large, flat plain) which has been affected by karstification and tectonism. It is extended in an E-W direction with a mean altitude of +95 m above sea level. Land use has been changed over the last 100 years. Originally the Kopaida was a marshy region, with the environment frequently changing between a periodic lake and a swamp. The last few years, the entire region has been drained and since then the fertile parts are under extensive agricultural practices.

*E-mail: evtziritis@geol.uoa.gr

The geology of the area is mainly characterized by karstic formations and a thick sequence of Quaternary deposits. The underlying older Alpine substrate consists of a succession of Triassic dolostones and dolomitic limestones, a Jurassic tectono-volnanic complex composed of schists, sandstones and ultrabasic blocks, a Cretaceous sequence of pelagic limestones which hosts locally Fe-Ni rich ores and finally the typical Eocene flysch [1]. The Post-Alpine sediments have a great thickness and form a succession of clays, breccias, sandstones, lacustrine marls of Plio-Plistocene age, and a few lignitic intercalations. The upper sequence consists of Quaternary fluvial phases [1, 2].

The existence of Fe-Ni-rich ores has been reported and located in several studies in the wider area of Kopaida [3–6]. They occur in outcrop only in the northeastern extrem-

ities of the area (Aghios Ioannis) (Figure 1 and 2) but their presence in the substrate of eastern Kopaida is significant due to the specific tectonic conditions [5].

Kopaida region belongs to the great hydrologic system of the Viotikos Kifisos River. The aquifers of the study area have formed according to the specific geological and tectonic conditions. The stratigraphic contacts between formations of different permeabilities as well as the tectonic nappes and the various deformation episodes, formed three individual aquifers. The upper one is developed in the Cretaceous limestone and is characterized by high permeability and karstic flow. The middle aquifer is developed in Jurassic limestones with elevated values of hydraulic conductivity, and the lower one is found in dolostones and dolomitic limestones. It is differentiated from superincumbent aquifers due to the considerable decrease of permeability and karstic development. The general groundwater flow is towards east, with local differentiations. Piezometric level is variable, ranging between 20m and 160m depending on local lithologic and tectonic conditions [7]. Discharges vary between 40 km^3/h and 300 km^3/h, depending on the type of the aquifer. Finally, the alluvial aquifer is of minor importance and is not included in this study.

The soils are characterized by a red or brownish-red color, with a heavy texture and frequent presence of breccias. They mainly consist of non-evoluted calcareous lacustrine sediments and therefore are classified as "Typic Haplaquent" in most of the cases, while a minor part of them is classified as "Mollic Haplaquent" [8]. The presence of root systems is common and the boundaries among the different horizons are abrupt and wavy. Soil structure and cohesion create satisfactory conditions for plant growth and biological activity.

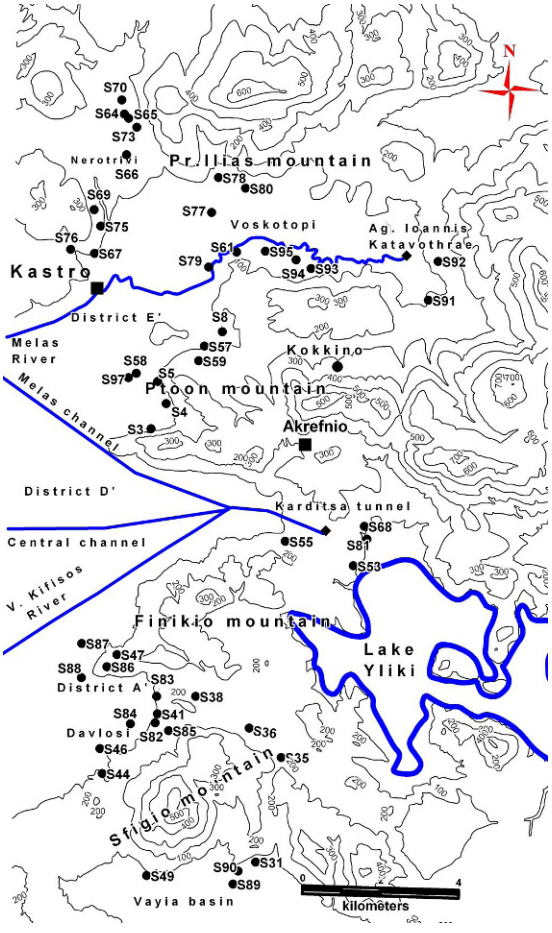

Figure 1. Sites of groundwater samples.

2. Methods and materials

2.1. Sampling and analysis

Seventy samples of both groundwater and soil were collected during field work, namely 50 samples of groundwater and 20 samples of soil. Groundwater samples were collected from all available boreholes of the karstic aquifer (Figure 1). During sampling all necessary precautions were taken in order to avoid any possible contamination. From the groundwater samples 28 parameters were determined (Table 1), including major ions (Ca^{2+}, Mg^{2+}, K^+, Na^+, Cl^-, NO_3^-, SO_4^{2-}, PO_4^{3-} and HCO_3^-), trace elements (Br, Cr, Fe, Ni, Mn, Ba, B, Si, Co, Cu, Cd and Zn) and physicochemical parameters (pH, EC and TDC) that were measured in situ. Data quality was assured by the introduction of internal reference samples and by analyzing duplicates of 10 samples. The precision was calculated and found according to the international standards.

Soil samples were collected from an area covering approximately 100 km^2 (Figure 2), with the use of an auger sampler from a depth of 30 cm. Surface debris, vegetation and the A-soil horizon was removed before sampling. The samples were digested with a mixture of $HClO_4$-HNO_3-HCl-HF and analyzed with an ICP-MS for the following 13 parameters: Al, Ba, Ca, Cu, Cr, Fe, K, Mg, Mn, Na, Ni, Pb and Zn. Data quality was assured by introduction of internal reference samples and by analyzing the duplicates of 5 samples. The precision was calculated from these duplicates and it was in accordance with the international standards. The results are shown in Table 3.

2.2. Statistical processing of data

For the initial assessment of the factors that control soil geochemistry, analytical data were statistically processed.

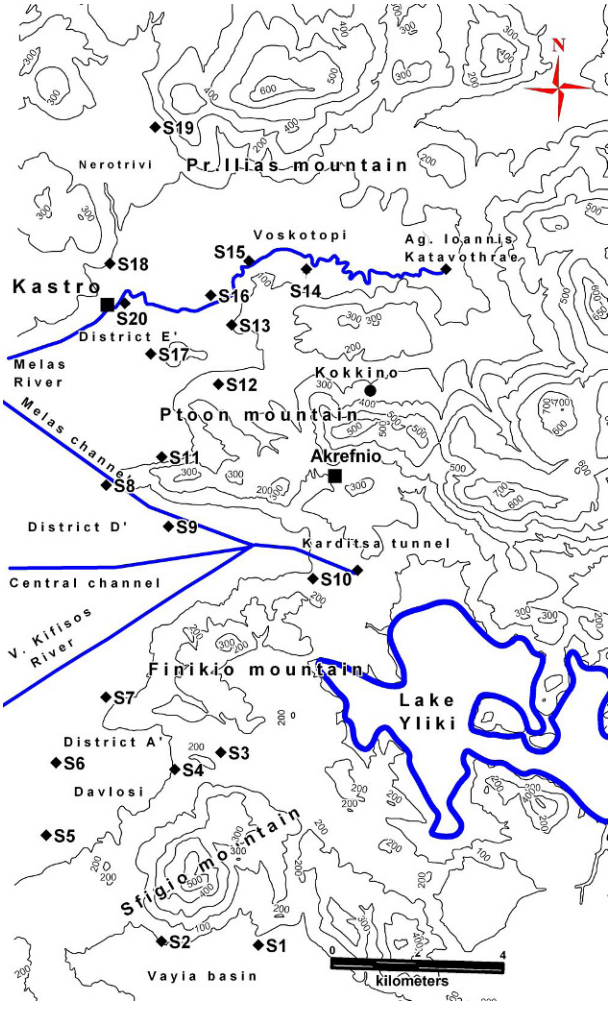

Figure 2. Sites of soil samples.

A cluster analysis was performed on a hierarchical amalgamate technique based on the Euclidean distance, for the extraction of possible links between the parameters (variables) of the soil samples. Prior to statistical analysis data was standardized by means of: $K_{ij}=(X_{ij}-X)/S_{ic}$ (1), where K_{ij} is the normalized value for X_{ij}, the i^{th} variable for the j^{th} sample, X is the mean value of i^{th} variable and S_{ic} is its standard deviation [9]. This process gives equal weight to each parameter. As it is already mentioned, the measure of similarity (correlation) is simply the distance as defined in Euclidean space [10]. The distance between two samples (j, k) is given by: $d_{ij} = \left[\sum_{i=1}^{N}\left(K_{ij}-K_{ik}\right)^2\right]^{1/2}$ (2) where K_{ik} the K_{th} variable measured on object i, K_{jk} is the K_{th} variable measured on object i. The data were classified in a relatively simple and direct manner with the results being presented as a dendrogram (Figure 6).

3. Discussion of geochemical results

3.1. Groundwater

The major processes that control the hydrogeochemical conditions were assessed by the results of chemical analyses (Table 1), spatial distribution of samples, and the existing literature. The influence from the calciferous formations in the wider area is significant, as it can be concluded from the elevated concentrations of Ca^{2+} and HCO_3^- for most of the samples. The typical average concentration of calcium in karstic systems is about 75 ppm [11]. Based on Table 1, the mean value of Ca^{2+} in the groundwater samples is about 96 ppm, denoting enrichment due to calcite dissolution. Furthermore, the ionic ratios (Table 2) of Mg^{2+}/Ca^{2+} for most of the samples vary between 0.5 and 0.7, denoting the impact from a calciferous aquifer [12, 13].

The contribution of the dolomitic aquifer is significant, as is seen in the elevated values of Mg^{2+} in some of the samples (S47, S64, S66, S81, S82, S84, S88 and S90). The Triassic dolostone is not the only origin of Mg^{2+} enrichment in the area, since there are also occurrences of other Mg-rich formations, such as the ophiolitic blocks of the Jurassic tectono-metamorphic complex. The distinction between these two sources can be seen in the ionic ratios of Mg^{2+}/Ca^{2+}(Table 2), which in the case of dolomitic aquifer ranges between 0.7-0.9, while in the case of ultrabasic formations it is greater than 0.9 [12, 13]. Apart from the ophiolitic blocks, the impact of the ultrabasic formations to groundwater chemistry derives also from the lateritic horizons. These can be assessed by the concentrations of some trace elements which are related to these stratigraphic horizons. More specifically, the elevated values of Fe and Mn (S44, S46, S47, S87, S88 and S89) are mostly related to the ophiolitic blocks, while the increase in the concentrations of Cr and Ni denote the impact from the lateritic horizons.

A major influence to groundwater geochemistry seems to derive from the local reducing conditions. It is well described [12, 14] that under anoxic conditions, the chemical parameters of NO_3^-, Fe^{3+} and Mn^{4+} could participate in the redox process, and act as oxidants. As a result, the above parameters will be removed from the solution, which will be enriched in Fe^{2+}, Mn^{2+} and nitrogen due to reduction [12, 15]. The above process is not instant, because the enrichment is achieved after the end of denitrification with the aid of bacterial catalysis [16]. This process is sufficient to interpret the geochemical status of the boreholes which are situated in Davlosi area (Figure 1) (SW part of the study area). The boreholes in this area have

Table 1. Chemical analyses of the groundwater samples (part 1, samples S4-S68; part 2, samples S69-S97).

		S3	S4	S5	S8	S13	S31	S35	S36	S38	S41	S44	S46	S47	S49	S53	S55	S57	S58	S59	S61	S64	S65	S66	S67	S68
Ca	ppm	152	98	69	131	95	82	86	91	76	98	103	159	111	86	69	81	77	109	92	95	59	81	38	92	78
Mg	ppm	54	37	37	39	15	25	21	21	23	32	27	42	57	25	35	35	33	88	39	90	44	40	99	51	38
K	ppm	2	2	2	2	1	12	1	1	2	2	2	4	2	3	2	1	2	2	2	2	1	2	1	1	1
Na	ppm	44	24	40	19	17	87	21	26	29	30	28	32	9	58	37	20	20	57	25	73	14	28	38	27	19
Cl	ppm	29	25	22	36	8	103	17	19	13	14	19	22	13	70	17	18	16	86	20	124	19	28	28	29	26
NO_3	ppm	66	22	4	55	25	22	28	22	38	52	21	4	5	27	23	65	28	24	28	7	20	17	55	39	28
SO_4	ppm	230	75	84	112	13	52	15	16	32	47	164	285	61	35	22	26	37	217	39	256	11	32	64	87	81
PO_4	ppm	0.70	0.52	0.08	0.16	0.29	0.08	1.19	0.65	0.1	0.14	0.16	0.13	0.69	0.14	0.15	0.09	0.38	0.2	0.15	0.44	0.22	0.22	0.42	0.33	0.4
HCO_3	ppm	282	250	205	220	277	253	220	250	273	224	269	370	284	200	264	245	278	361	306	391	260	273	428	287	256
Al	ppb	3	21	29	21	9	11	22	4	32	17	29	4	4	4	18	6	26	4	10	8	9	7	13	10	4
As	ppb	0	1	0	2	0	2	0	0	0	1	0	1	3	1	1	1	1	1	1	1	2	1	2	1	1
B	ppb	21	22	16	0	20	74	20	20	26	24	25	23	21	48	25	27	20	34	21	27	0	0	35	0	28
Ba	ppb	68	89	65	45	13	24	30	31	78	38	69	61	120	18	39	43	32	73	35	70	24	23	45	45	26
Br	ppb	55	53	79	59	47	423	94	80	103	76	122	125	77	255	76	69	40	153	58	185	93	64	137	63	89
Cd	ppb	1	0	0	0	0	0	2	0	1	1	1	0	0	0	1	0	0	1	1	2	3	2	6	2	0
Cr	ppb	2	0	0	1	3	2	1	1	1	2	1	2	0	5	12	6	2	2	3	1	5	8	33	5	15
Co	ppb	0	2	5	6	4	11	3	3	2	9	6	11	1	2	2	2	2	8	5	2	2	1	2	4	1
Cu	ppb	2	3	4	5	11	6	5	2	6	5	5	1	2	2	10	2	4	5	2	2	6	2	2	4	1
Fe	ppb	3	2	3	13	1	4	5	13	3	6	2	550	3	24	2	0	4	3	4	20	8	20	2	6	0
Mn	ppb	8	5	14	1	1	2	5	1	37	3	260	380	750	1	4	1	3	1	2	24	1	3	1	3	0
Mo	ppb	1	1	1	1	0	1	0	0	1	0	0	0	5	1	1	1	1	1	1	1	1	1	1	1	0
Ni	ppb	4	1	0	6	8	2	2	1	1	1	5	1	6	1	3	0	8	3	2	2	1	14	1	2	0
Si	ppm	7.5	7.5	7.0	5.8	7.0	10.5	5.8	5.5	6.0	6.1	8.0	8.4	8.9	8.2	4.6	5.9	9.5	7.5	8.7	6.9	10.4	7.8	16.4	6.9	9.7
Pb	ppb	0	0	2	1	1	0	2	1	0	1	0	0	1	1	2	0	0	0	2	0	1	1	0	0	0
Zn	ppb	50	11	5	19	110	12	27	8	366	8	64	6	15	37	50	22	57	13	221	210	142	20	15	80	26
EC	µS/cm	960	850	700	870	580	960	510	560	610	680	720	990	820	670	610	610	670	1210	680	1300	570	600	980	830	330
TDS	mg/L	480	420	350	430	280	470	250	280	300	340	490	500	410	330	300	300	330	600	340	650	290	300	490	410	320
pH		7.9	7	7.5	7	7.6	7.6	7.6	7.7	7.6	7.9	7.5	7.3	8	8.1	8.1	7.9	7.9	8.2	7.9	8.2	8.2	8.1	8.3	7.9	7.3

		S69	S70	S73	S75	S76	S77	S78	S79	S80	S81	S82	S83	S84	S85	S86	S87	S88	S89	S90	S91	S92	S93	S94	S95	S97
Ca	ppm	100	81	82	103	92	88	82	85	77	92	138	90	80	92	112	126	136	95	101	162	82	81	81	97	127
Mg	ppm	43	43	38	43	35	50	38	46	50	31	39	32	59	26	42	82	81	32	27	24	34	39	34	44	64
K	ppm	1	1	1	2	1	1	1	2	1	3	2	2	3	1	2	5	4	8	5	1	1	2	1	2	2
Na	ppm	19	28	11	18	10	20	12	24	19	35	23	14	38	15	14	24	25	145	89	14	14	16	14	16	67
Cl	ppm	19	27	19	23	12	43	24	36	33	50	27	16	59	20	18	23	24	191	143	45	28	28	23	26	117
NO_3	ppm	33	42	15	31	19	46	27	16	38	20	78	10	4	27	6	3	3	20	22	12	13	16	17	27	8
SO_4	ppm	41	51	7	36	5	48	14	24	37	21	63	16	2	27	64	32	326	71	49	52	44	39	16	43	169
PO_4	ppm	0.26	0.36	0.36	0.23	0.26	0.13	0.13	0.16	0.2	0.12	0.15	0.08	0.09	0.13	1.1	0.21	0.17	0.07	0.06	0.78	0.82	0.16	0.33	0.51	0.15
HCO_3	ppm	295	241	307	277	301	285	274	205	290	277	295	293	383	254	405	532	481	205	256	331	220	282	280	272	381
Al	ppb	6	20	16	33	11	7	4	8	10	16	22	8	19	46	12	18	13	23	8	10	6	4	6	4	5
As	ppb	1	1	1	1	1	1	2	1	0	1	1	0	3	1	1	2	5	3	2	0	1	1	1	1	2
B	ppb	26	16	0	22	15	0	0	28	0	40	28	28	51	26	27	33	32	125	81	0	0	0	15	21	49
Ba	ppb	17	20	27	25	23	23	12	37	25	45	54	24	146	34	74	93	107	25	21	35	25	29	24	26	130
Br	ppb	126	111	75	85	53	69	75	100	78	166	108	59	146	77	86	138	137	655	437	110	91	50	56	91	260
Cd	ppb	0	0	1	1	0	2	0	2	2	8	0	4	4	2	3	3	2	0	1	42	4	1	2	1	1
Cr	ppb	12	6	9	6	6	5	4	6	4	5	5	1	1	3	1	1	1	3	2	16	10	2	3	7	1
Co	ppb	7.4	3.4	3.5	7.4	5.8	2.9	11.2	1.7	5.5	2.5	11.3	1.2	1.8	1.6	2.2	1.6	2.4	3.2	1.8	2.7	1.7	1	3.2	2	2.4
Cu	ppb	4	3	4	7	6	3	11	2	6	3	11	1	2	2	2	2	2	3	2	5	2	1	3	2	2
Fe	ppb	15	3	158	51	3	152	151	129	147	202	30	154	162	235	220	263	818	6	211	245	218	132	17	184	236
Mn	ppb	2	2	1	4	0	1	0	4	1	1	2	0	85	1	301	252	285	1	1	6	1	0	1	4	72
Mo	ppb	0	1	1	0	1	1	0	2	1	0	0	0	10	0	2	1	2	1	1	0	1	1	1	1	2
Ni	ppb	2	4	0	1	0	1	0	2	0	1	1	0	1	0	3	3	0	1	0	6	0	0	0	1	1
Si	ppm	11.1	12.4	6.6	10.0	6.5	6.4	6.5	6.0	6.8	7.7	10.6	5.9	11.9	7.7	7.9	14.3	15.5	6.5	6.0	5.4	6.3	6.9	6.9	9.8	7.7
Pb	ppb	1	0	0	0	0	0	0	0	0	0	2	0	1	0	0	0	0	0	0	1	1	0	0	0	0
Zn	ppb	16	20	26	16	20	31	13	49	48	63	56	10	77	274	12	13	15	20	21	424	61	8	35	9	109
EC	µS/cm	650	770	600	680	560	750	590	670	700	680	800	580	830	580	720	1000	1090	1130	920	680	530	610	590	620	1160
TDS	mg/L	320	380	290	340	270	370	290	330	350	330	390	290	410	280	350	500	540	560	460	340	260	300	290	320	580
pH		7.8	8.1	8.1	7.9	8.1	8	8.2	7.9	8	8.3	7.5	7.5	7.8	7.7	7.4	7.8	7.3	7.9	7.6	7.7	7.8	7.6	7.8	7.7	7.4

common haracteristics, such as elevated values of Fe (220-818 ppb) and Mn (252-750 ppb). Also, these boreholes have low concentrations of NO_3^- (2.7-7.5 ppm), considering the background value (22 ppm) for nitrates in the wider area, land use (extended agricultural practices), and the nitrate values of the neighbouring boreholes which are significantly higher (38-78 ppm). The possible interpretation of this phenomenon could be attributed to the existence of local reducing conditions. These conditions are developed due to the concentrated amount of organic material which occurs in the Quaternary deposits. The marshy conditions of the former Lake of Kopaida gave rise to lacusrtine phases which were enriched in organic content and characterized by diminished oxygen concentrations and nitrates to nitrogen reduction.

Table 2. Ionic ratios and water types of the Kopaida groundwater samples.

Sample	Mg/Ca	SO_4/Cl	Type	Sample	Mg/Ca	SO_4/Cl	Type
S3	0.6	5.76	Ca-SO_4	S69	0.7	1.54	Ca-HCO_3
S4	0.6	2.20	Mg-HCO_3	S70	0.9	1.38	Ca-HCO_3
S5	0.9	2.83	Ca-HCO_3	S73	0.8	0.27	Ca-HCO_3
S8	0.5	2.33	Ca-HCO_3	S75	0.7	1.16	Ca-HCO_3
S13	0.3	1.27	Ca-HCO_3	S76	0.6	0.31	Ca-HCO_3
S31	0.5	0.37	Ca-HCO_3	S77	0.9	0.82	Ca-HCO_3
S35	0.4	0.66	Ca-HCO_3	S78	0.8	0.43	Ca-HCO_3
S36	0.4	0.63	Ca-HCO_3	S79	0.9	0.49	Ca-HCO_3
S38	0.5	1.82	Ca-HCO_3	S80	1.1	0.83	Mg-HCO_3
S41	0.5	2.48	Ca-HCO_3	S81	0.6	0.31	Ca-HCO_3
S44	0.4	6.54	Ca-HCO_3	S82	0.5	1.72	Ca-HCO_3
S46	0.4	9.56	Ca-SO_4	S83	0.6	0.74	Ca-HCO_3
S47	0.8	3.41	Ca-HCO_3	S84	1.2	0.03	Mg-HCO_3
S49	0.5	0.37	Ca-HCO_3	S85	0.5	1.00	Ca-HCO_3
S53	0.8	0.98	Ca-HCO_3	S86	0.6	2.62	Ca-HCO_3
S55	0.7	1.08	Ca-HCO_3	S87	1.1	1.03	Mg-HCO_3
S57	0.7	1.66	Ca-HCO_3	S88	1.0	10.02	Ca-HCO_3
S58	1.3	1.87	Mg-HCO_3	S89	0.6	0.27	Na-Cl
S59	0.7	1.44	Ca-HCO_3	S90	0.4	0.25	Ca-Cl
S61	1.6	1.53	Mg-HCO_3	S91	0.2	0.86	Ca-HCO_3
S64	1.2	0.42	Mg-HCO_3	S92	0.7	1.15	Ca-HCO_3
S65	0.8	0.82	Ca-HCO_3	S93	0.8	1.03	Ca-HCO_3
S66	4.3	1.67	Mg-HCO_3	S94	0.7	0.51	Ca-HCO_3
S67	0.9	2.23	Ca-HCO_3	S95	0.7	1.22	Ca-HCO_3
S68	0.8	2.30	Ca-HCO_3	S97	0.8	1.07	Ca-HCO_3

The karstic aquifers which lie to the east of the study area are influenced by saline waters, mainly due to the over-exploitation of boreholes [1]. Similar process seems to be valid in the region of Vayia (Figure 1), where the seawater related parameters of Na^+, K^+, Cl^-, SO_4^{2-} and Br are locally higher than the others. The above assessment is verified by the elevated values of EC and TDS, which exceed 1000 μS/cm and denote possible seawater impact [17]. The ionic ratios of SO_4^{2-}/Cl^- (0.25-0.37) (Table 2) for the boreholes of the Vayia area (S31, S89 and S90) show values close to seawater (≈0.0524) [16]. Finally, the sequence of Na-Cl and Ca-Cl water types (Table 2) for the boreholes S89 and S90 (Figure 3), is typical for regions under saline impact, denoting cation exchange between Ca^{2+} and Na^+ [11, 19].

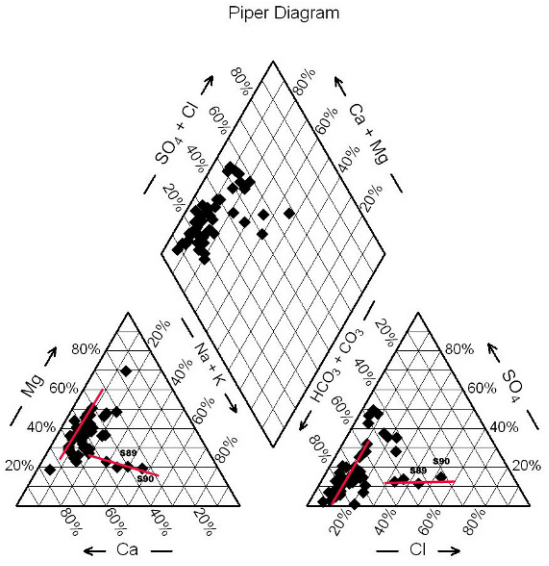

Figure 3. Piper diagram for the groundwater samples.

The Piper diagram illustrates that two theoretical trends can be distinguished (Figure 3). The primary one connects Ca^{2+} with Na^+ members, and the secondary one connects Ca^{2+} with Na^+-K^+ members. The possible interpretation for the major trend could be the depiction of the wide range of samples stemming from different aquifers with variable concentrations of Ca^{2+} and Mg^{2+}(Jurassic or Cretaceous limestone aquifers or Triassic dolomitic aquifer). The secondary trend occurs only in the boreholes (S31, S49, S89 and S90) which are situated in the south-eastern part of the area (Figure 1), and denotes the cation exchange process between Ca^{2+} and Na^+, which occurs progressively towards groundwater flow to east.

The existence of five different water types is suggested (Table 2). The dominant water type is Ca-HCO_3 which reflects the samples that originate from the karstic system. The impact from the dolomitic aquifer and the Mg-rich ultrabasic formations is reflected in the water type of Mg-HCO_3. The final three water types are Ca-SO_4, Na-Cl and Ca-Cl. The water type of Ca-SO_4 appears only in two samples, but an important assessment is made through the sequence of the Na-Cl and Ca-Cl water types, which verifies the approach of the saline plume, denoting cation exchange [19] between Ca^{2+} and Na^+ as has already been discussed.

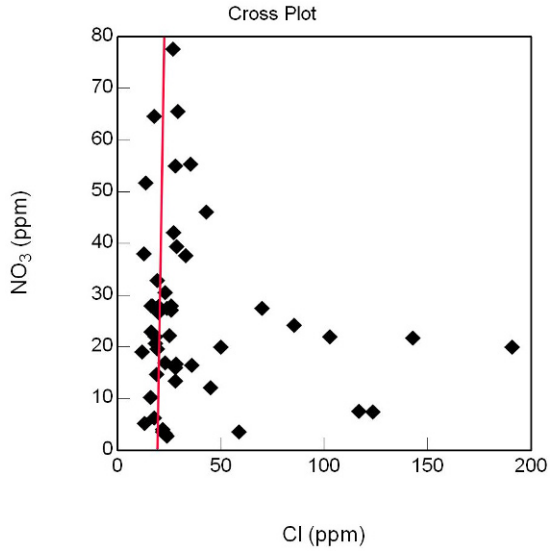

Figure 4. Cross plot between NO_3^- and Cl^- with the addition of the theoretical regression line.

The last impact to groundwater chemistry derives from manmade activities. Based on field observations and chemical analyses (Table 1), the manmade impact is significant through the elevated values of NO_3^- (S8, S38, S41, S55, S66, S67, S70, S77, S80 and S82). The origin of nitrates should be attributed exclusively to nitrate fertilizers, since the other possible factors for NO_3^- enrichment don't seem to exist or affect groundwater chemistry at all. In more detail the possible oxidation of nitrogen in the organic sediments could not lead to the results such as those measured and observed, in terms of elevated concentrations and spatial distribution. Furthermore, there are no occurrences of nitric salts of evaporitic origin. Finally, the origin of NO_3^- form sewage effluents or septic tanks should be excluded because there is no correlation between NO_3^- and other parameters such as Cl^- or HCO_3^-. A correlation between NO_3^- and Cl^- with values higher than + 0.35 denotes the common source of these two parameters which should be attributed to municipal or industrial wastes [20]. As can be conducted from Figure 4, the correlation between NO_3^- and Cl^- is non linear (r^2=0.025), indicating no common source of these chemical parameters.

4. Soils

Soil chemical analyses (Table 3 and Figure 5) reveal that the elevated values of Ca^{2+} (S6, S8, S9, S14, S15, S16, S17 and S20) reflect the influence of the prevailing weathered carbonate formations. The ongoing process of karstification seems to be dominant, resulting to $CaCO_3$ enrichment of the soil horizons. The Mg^{2+} content shows elevated values in samples S1, S2, S13, S18 and S19, and seems to have a dual origination. The main source derives from the Triassic dolostones of the Alpine substrate, but there is also a profound influence from the ultrabasic formations of the tectono-metamorphic melange.

Table 3. Chemical analyses of the soil samples.

Element	Ca	Mg	K	Na	Al	Ba	Co	Cu	Cr	Fe	Mn	Ni	Pb	Zn
Sample	%	%	%	%	%	ppm	ppm	ppm	ppm	%	ppm	ppm	ppm	ppm
S1	14.7	2.0	0.7	0.2	3.7	238	31	32.7	399	3.8	814	400	11.8	69
S2	7.0	2.0	1.2	0.3	5.5	481	35	27.9	370	4.9	865	476	26.9	108
S3	3.2	0.5	0.6	0.7	2.6	231	12	38.8	486	1.7	260	124	10.4	38
S4	1.4	0.8	0.8	0.7	3.3	764	18	10.6	740	2.3	477	156	32.2	107
S5	7.2	1.5	1.1	0.8	4.0	302	25	25.4	422	3.3	705	267	14.8	66
S6	21.2	1.1	0.5	0.3	2.2	1294	11	27.9	135	1.8	554	125	54.4	106
S7	11.5	0.8	0.9	0.6	4.1	269	12	18.3	276	1.9	221	160	16.4	74
S8	26.5	0.9	0.3	0.2	1.4	979	6	26.4	69	1.1	391	74	55.4	114
S9	20.6	0.9	0.6	0.3	2.5	278	10	15.4	129	1.4	258	112	21.4	48
S10	15.2	1.1	0.9	0.5	3.8	734	20	18.5	196	3.0	401	222	30.6	87
S11	8.6	1.8	1.1	0.4	5.2	315	13	19.3	248	2.9	186	168	20.6	94
S12	10.5	1.3	1.1	0.4	5.4	1665	22	20.1	236	3.6	601	217	65	157
S13	12.8	2.2	0.9	0.3	4.0	848	14	30.6	211	2.6	261	145	38.3	104
S14	31.0	0.6	0.2	0.1	0.9	1760	4	10.2	42	0.6	263	53	63	110
S15	22.5	1.1	0.5	0.1	2.8	199	13	13.2	163	1.9	278	179	9.7	39
S16	32.9	0.7	0.2	0.0	0.7	2733	4	11.7	39	0.6	346	49	95.5	177
S17	33.8	0.6	0.1	0.0	0.7	344	3	6.8	37	0.5	506	43	12.9	26
S18	13.7	2.2	0.7	0.3	3.5	320	40	23.1	587	3.8	600	547	20.3	73
S19	6.0	2.9	1.1	0.2	5.3	275	63	31.2	1458	6.6	1217	926	22.1	95
S20	24.7	1.2	0.4	0.1	2.3	684	14	14	153	1.8	353	197	27.4	70

However, the elevated values of Cr (S1, S3, S4, S5, S18 and S19) and Ni (S1, S2, S5, S10, S12, S18 and S19) originate from the lateritic horizons. Their presence is significant at the north-eastern part of Kopaida. Specifically, sample S19 is clearly influenced by this factor revealing the lateritic impact in the region, since it has elevated values for Cr, Mn, Fe, Ni, Co and low for Ca. The above assessment is in accordance with the geological background, as the Fe-Ni rich ores occur between the statigraphic contact of the Jurassic and Cretaceous limestones, where the sample is sited. An interesting assessment is made through the high values of Ba (S6, S8, S12, S14 and S16) which probably owe their elevated concentrations to a potential sulfide mineralization along with Pb and Zn, related to the ophiolitic blocks of the Jurassic melange. As it can be conducted by the map of Figure 5, there is no correlation between the geological background and the elevated values of Ba. Additionally, the elevated values show no specific spatial distribution. For example, the neighbouring samples S14, S15 and S16, have a great

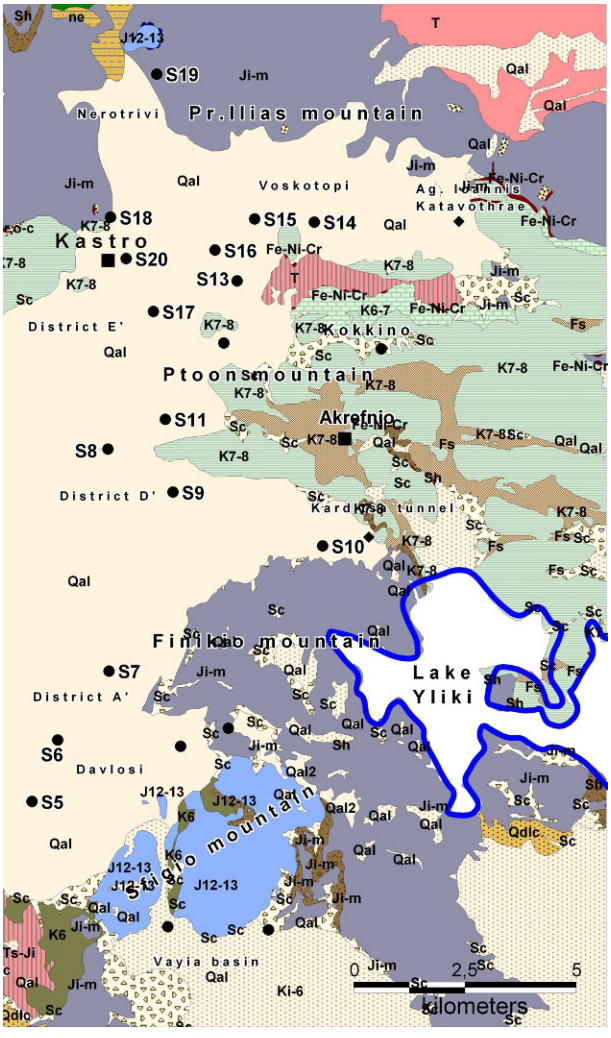

Figure 5. Soil sampling sites and detailed geological map of the study area. (Map legend- Qal: Alluvial deposits, Sc: Scree and talus cones, Qdlc: Neogene formations, Fe-Ni-Cr: Lateritic horizons, T: Triassic dolostones, Ji-m and J_{12-13}: Jurassic limestones, Sh: Tectono-metamorphic complex, K_6 and K_{7-8}: Cretaceous limestones, Fs: Flysch.

variation in Ba concentrations, denoting the impact from local factors and specific geospatial conditions.

The dendrogram is interpreted to be classified into three groups. The first group includes the variables Al, Fe, Ni, Mg, Cr and Mn denoting the correlation due to Cr-Ni-Fe ores. The second includes the variables Ba, Pb and Zn denoting the correlation due to the ultrabasic formations of the schist-sandstone sequence, along with the presence of a weak sulfide mineralization. Finally the existence of an individual variable (Ca), reflects the karstic geological environment (limestones).

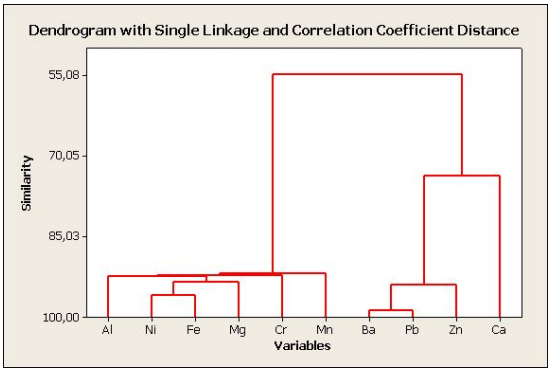

Figure 6. Dendrogram with single linkage and correlation coefficient distance for the variables of the 20 soil samples.

5. Conclusions

The Kopaida plain is a widely cultivated region with significant geological characteristics, due to the presence of an extended karstic substrate and a thick succession of Quaternary deposits above it. The geochemical conditions of groundwater originate both from manmade and natural factors. The manmade factors are related with the agricultural activities and the extended use of nitrogen fertilizers, as well as the overexploitation of boreholes which created favourable conditions for the approach of a saline water plume in the southeastern area. This plume doesn't seem to affect in a major way the qualitive characteristics of groundwater, but its approach can be verified by various assessments such as the elevated concentrations of the seawater related parameters, the sequence of water types and from the ionic ratio of SO_4^{2-}/Cl^-, which show values close to seawater for the samples of the southeastern part. The natural factors that affect groundwater chemistry derive from the specific geological conditions. The impact from the ultrabasic formations of the Jurassic tectono-metamorphic complex and from the lateritic horizons is profound, expressed through the locally elevated concentrations of Mn, Fe and Ba as well as in the minor increase in the concentrations of Cr and Ni. Furthermore, the organic rich sediments gave rise to reducing conditions, which altered the initial geochemical status of groundwater, resulting either to depletion or to enrichment of chemical parameters (Mn, Fe and NO_3^-). Conversely, the parameters that seem to control the geochemistry of soils derive exclusively from natural factors, such as the geological formations and their weathering rates. The results from chemical analyses and statistical process revealed that the major factor is the weathering of lateritic horizons and karstic substrate.

A weak sulfide mineralization was also assessed through

the correlation of Ba, Pb and Zn. The influence of the sulfide mineralization can also be distinguished in groundwater through the local elevated values of Ba and Zn in some of the samples, except from Pb which is practically immobile in slightly alkaline environments, conditions that do exist in the study area. This could also be attributed the fact that Cr or Ni concentrations are not elevated in groundwater, despite the existing local enrichment of soils due to lateritic weathering.

References

[1] Pagounis M., Gkertzos T., Gkatzoyiannis A., Hydrogeological study of Viotikos Kifisos basin. 1994, Technical report, I.G.M.E (in Greek)

[2] Allen H.D., Late Quaternary of the Kopais Basin, Greece: Sedimentary and Environmental History, PhD thesis, University of Cambridge, England, 1986

[3] Paraskevaidis I., The geology of the area Lakes Yliki and Paralimni: Review of former and recent evidences, Technical Chronicles, 1972, 3, 11-27 (in Greek)

[4] Koumantakis I., New evidences about the Fe-Ni-rich ores of Yliki, Annales Geologique, Des Pays Hellinique, 1975, 7, 34-55

[5] Albantakis N., Koundouros D., Nickel minerals of the Eastern Greece geotectonical unit, Mineral Wealth, 1984, 31, 22-37

[6] Albantakis N., Discover and trace of Fe-Ni-rich ores in Kopaida with the use of geomagnetic methods and boreholes, Mineral Wealth, 1984, 31, 12-25

[7] Tziritis E.P., Kelepertzis A., Stamatakis M.G., Hydrogeochemical and environmental conditions of East Kopaida-Yliki karst groundwater system, 8th International Hydrogeological Congress, Athens-Greece, 2008, 2, 733-742

[8] Theocharopoulos S., Karagianni M., Christou P., Gkatzogianni P., Afentaki A., Aggelidis S., Diachronic notes in inorganic nitrogen concentrations in the cultivated regions of Kopaida soils and waters, Geotechnical Scientific Issues, 1995, 4

[9] Hussein M., Hydrochemical evaluation of groundwater in the Blue Nile basin, eastern Sudan, using conventional and multivariate techniques, Hydrogeol. J., 2004, 12, 144-158

[10] Eriksson E., Principles and application of hydrochemistry, Chapman & Hall, UK, 1985

[11] Appelo C. and Postma D., Geochemistry, groundwater and pollution, 2nd edition, A.A. Balkema Publishers, The Netherlands, 2005

[12] Kim J., Kim R., Lee J., Chang H., Hydrogeochemical characterization of major factors affecting the quality of shallow groundwater in the coastal area at Kimje in South Korea, Environ. Geol., 2002, 44, 478-189

[13] Zhu G.F., Li Z.Z., Su Y.H., Ma J.Z., Zhang Y.Y., Hydrogeochemical and isotope evidence of groundwater and recharge in Minqin Basin, Northwest China, J. Hydrol., 2007, 333, 239-251

[14] Gascoyne M., Evolution of Redox conditions and groundwater composition in recharge-discharge environments on the Canadian Shield, Hydrogeol. J., 1997, 5

[15] Hounslow A., Water quality data: Analysis and interpretation, Lewis Publishers CRC press, New York, 1995, 397

[16] Lovely D., Microbial Fe(III) redox in subsurface environments, FEMS Microbiol. Rev., 1997, 20, 205-313

[17] Petalas C., Diamantis I., Origin and distribution of saline groundwaters in the upper Miocene aquifer system, coastal Rhodope area, northeastern Greece, Hydrogeol. J., 1999, 7, 305-316

[18] Hem J., Study and interpretation of the chemical characteristics of natural water, U.S. Geological Survey, Water Supply Paper, 1985, 2254

[19] Al-Ruwaih, Chemistry of groundwater in the Dammam aquifer, Kuwait, Hydrogeol. J., 1995, 3

[20] Pacheco J., Marin L., Cabrera A., Steinich B., Escolero O., Nitrate temporal and spatial patterns in 12 water-supply wells, Yucatan, Mexico, Environ. Geol., 2001, 40, 708-715